The use of thermal mapping in evaluation of mechanically induced electrical degradation of graphene - based transparent heaters

Anna Kozłowska[1], Grzegorz Gawlik[1], Anna Piątkowska[1], Aleksandra Krajewska[1], Wawrzyniec Kaszub[1]

The purpose of this study is to investigate temperature distributions of graphene-based transparent heaters deposited on glass. Furthermore it analyses the influence of layer discontinuities such as scratches and cracks on the performance of Joule-heated samples. Graphene mechanical strength was examined by the nanoscratch method at incremental loads using a ball on a flat sample surface. In the case of the controlled load several scratches were produced on the graphene surface. Tribological tests were conducted at different constant loads. The paper presents scanning electron micrograph (SEM) observations of the modified graphene surface. Infrared imaging of Joule-heated samples indicates a significant uniformity deterioration of the thermal maps due to the current flow alteration in the presence of structural imperfections. The results obtained in the course of this study give new insight into the role of defects such as cracks or discontinuities in the overall performance of graphene transparent layers.

Key words: graphene, transparent layer, heating element, infrared imaging, thermal distribution, mechanical defect

Zastosowanie mapowania termicznego do oceny elektrycznej degradacji uszkodzonych mechanicznie grafenowych przezroczystych elementów grzejnych

W pracy przeprowadzone zostały badania rozkładów termicznych elementów grzejnych zawierających warstwy grafenowe naniesione na szkło. Analizowany był wpływ nieciągłości warstwy w postaci zarysowań i pęknięć. Mechaniczna wytrzymałość grafenu badana była za pomocą metody nano-zarysowań przy narastającym obciążeniu kulki oddziaływującej na płaską powierzchnię próbki. Przy zastoso-waniu kontrolowanego maksymalnego obciążenia wykonano szereg rys na powierzchni grafenu. Przeprowadzono testy tribologiczne dla różnych stałych obciążeń. W pracy zawarto wyniki analizy zmodyfikowanej powierzchni grafenu za pomocą skaningowego mikro-skopu elektronowego (SEM). Obrazowanie w podczerwieni próbek podgrzewanych za pomocą wydzielanego ciepła Joula wskazały na znaczne pogorszenie jednorodności rozkładów termicznych, na skutek zmiany drogi przepływu prądu w przypadku występowania niedoskonałości strukturalnych. Wyniki pozwalają na ocenę wpływu defektów w postaci pęknięć i nieciągłości na działanie przezro-czystych grafenowych warstw grzejnych.

Słowa kluczowe: grafen, warstwa przezroczysta, element grzejny, obrazowanie w podczerwieni, rozkład termiczny, defekt mechaniczny.

1. Introduction

Graphene attracts much interest because of its ability to conduct electric current of high density, almost uniform in the wide spectral range level of optical transparency, and because of its outstanding thermal properties. High optical transparency is particularly desirable for applications such as transparent screens, transparent Joule heaters integrated with glass windows [1 - 3], and photovoltaics or elastic displays [4]. Outstanding thermal properties such as high in-plane thermal conductivity make this material an ideal candidate for heat-spreading applications [5]. Structure variations (e.g. graphene wrinkles, grain boundaries), however, may introduce highly localized resistive heating and the rise of the temperature, both of which are likely to affect the reliability of graphene

devices [6]. Detrimental to the reliability is the presence of hot-spots, caused by the non-uniform current flow at the graphene layer discontinuities [7]. This effect leads to the accelerated degradation of the device, especially in the case of high current densities [8]. Although on a nanoscale, defect-free graphene is a robust material with an intrinsic strength reaching 42 N m^{-1} [9], in practical technical appli-cations, a single-layer graphene is rather fragile and easily damaged. However, the role of the defects in the form of discontinuities and cracks in the modification of thermal performance of graphene-based transparent heaters was thoroughly investigated. In the paper, we describe the thermal behavior of a Joule-heated graphene sample with induced discontinuities. Graphene mechanical strength was examined by the nanoscratch method at incremental loads and tribological tests at different constant loads with the use of a ball tip. Mechanical defects introduced in this

[1] *Institute of Electronic Materials Technology*, 133 Wólczynska Str., 01-919 Warsaw, Poland, e-mail: Anna.Kozlowska@itme.edu.pl

manner were analyzed using scanning electron microscopy (SEM). Joule-heating distributions of the modified graphene layers were examined using the high-resolution infrared imaging method.

2. Experimental

The graphene films were synthesized by chemical vapor deposition (CVD) on the surface of 35 μm thick copper foils. To obtain graphene on this material, we used the Aixtron Black Magic system with air-shower reactor. This kind of device ensures good stability and pyrometrically-controlled temperature and reasonable small thermal gradient effect. During the process we use pure (ultra high purity) hydrogen, argon and methane. In order to grow graphene on copper foil, the samples were heated up to 450°C (first step), 750°C and finally 960°C with presence of Argon and hydrogen. The growth of graphene was realized at 960°C and the methane flow with flow between 35 and 70 sccm during 12 minutes.

After the growth, the graphene on Cu foil was covered with a thin layer of poly (methyl-methacrylate) (PMMA) by a spin-coating method. This procedure prevents graphene film from destruction during the electrochemical delamination. A simplified scheme of this procedure is presented in the Fig. 1. After the electrochemical delamination, graphene with PMMA must be cleaned (RCA ceaning method) in deionized water and finally its covering dedicated substrate. Before removing PMMA, the samples were heated up to 120°C in a n air atmosphere. In the final step PMMA was removed into acetone and the sample was heated up once again up to 125°C. To characterize the graphene transferred onto the substrate, we performed

Fig. 2. Photograph of graphene-based heater deposited on glass plate.
Rys. 2. Fotografia grzejnika grafenowego nałożonego na szklaną płytkę.

Raman spectroscopy as well SEM and AFM imaging. An Auriga cross beam workstation from Carl Zeiss was used for SEM characterization of the graphene surface.

Ohmic contacts to graphene were formed using silver conductive paste. A photograph of an exemplary graphene-based transparent heater is shown in Fig. 2. The size of the sample was 25 mm x 20 mm. The tribological system consisted of a ball on a flat surface with normal load of 0.8 N. The counterpiece was formed by a ceramic ZrO_2 ball with a diameter of 2 mm. The one-stroke mode was applied in tribological tests for a better observation of the graphene wear phenomena. Several graphene discontinuities could be observed on the graphene surface. The position of these scratches on the sample is schematically shown in Fig. 3a.

Infrared imaging was performed using the InSb 640 M camera (Thermosensorik / DCG Systems). A wide-field lens with the focal length of 28 mm was employed in this work. During the tests, the sample was placed on the heated table to register the calibration maps in the controlled temperature.

The course of the study was as follows: a pristine graphene sample was first examined using the infrared imaging (thermographic) method. In the next step, the tribological tests were made and the sample was observed under SEM and optical microscopes. Then, the sample was again characterized thermally using the infrared imaging method.

Fig. 1. Essential steps in the process of graphene transfer (from left to right): electrochemical delamination, cleaning process, covering graphene with PMMA on isolating surface, hot-plate, PMMA removing, hot plate.
Rys. 1. Podstawowe kroki w procesie przenoszenia grafenu (od strony lewej do prawej): delaminacja elektrochemiczna, proces czyszczenia, pokrywanie grafenu za pomocą PMMA, podgrzewanie, usuwanie PMMA, podgrzewanie.

3. Results and discussion

The results of the thermographic characterization for a pristine, Joule-heated sample are presented in Fig. 3b-d. During the test, thermal maps were registered for the currents (I) ranging from 5.7 to 30.0 mA and the voltages (U) ranging from 10 to 50 V, resulting in the power surface density from 0.0114 W/cm^2 to 0.3 W/cm^2. An exemplary steady-state thermal map captured for $I = 30$ mA and $U = 50$ V is shown in Fig. 3b. It reveals the areas of elevated temperature located in the middle and the side part of the sample. In the upper part of the image, a distinct hot spot can be observed. Horizontal and vertical cross--sections through this hot spot for different supplied power levels are shown in Fig. 3c and Fig. 3d, respectively.

In the next step, as shown in the scheme in Fig. 3a, four scratches were made on the sample using the tribological system described in the previous section. SEM observa-

tions of the sample reveal different destruction mechanisms of the graphene layer depending on the applied load and on the adhesion of the graphene to the glass substrate. They are cohesive cracks, wrinkles formation under shear stress, delamination of the large graphene areas, destruction on folds, and tearing stripes, all of them leading to the formation of larger or smaller extended nonconductive areas, primarily in the form of scratches, which modify current flow in the graphene layer.

A SEM photograph of the tip of one of the scratches is presented in Fig. 4a. Apart from intentionally introduced cracks, observations of the sample indicate various defects such as the cracks, graphene discontinuities and wrinkles. Particularly, an ending point of a defect starting from the sample border can be observed at the position of the hot spot in the upper part of the sample (Fig. 4b). The sample with intentionally and accidentally introduced scratches was again characterized using the infrared imaging method. A thermal image captured for $U = 50$ V is shown
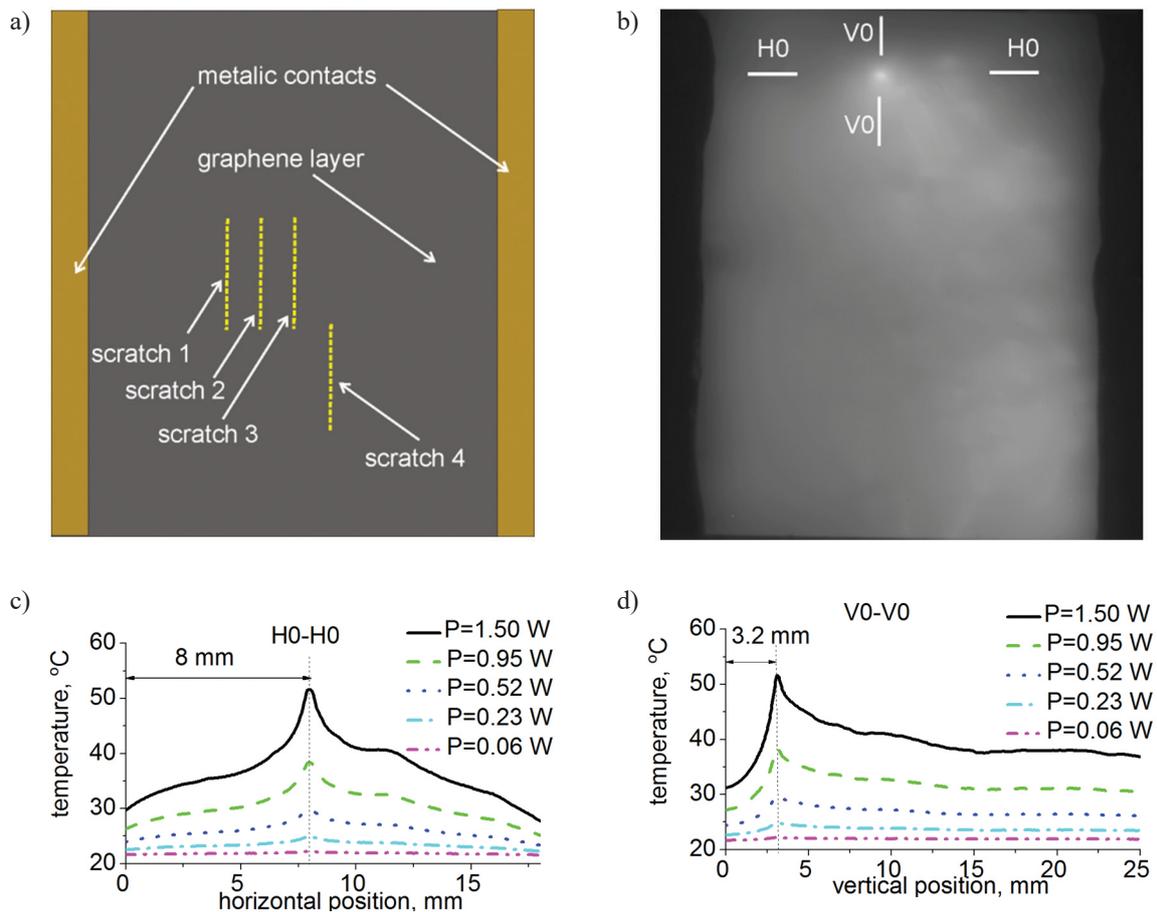
Fig. 3. Schematic of the sample and the results of the thermographic characterization of pristine CVD graphene sample. a) Drawing of the sample with the marked position of intentional scratches. b) Thermal image for a pristine sample biased with $I = 30$ mA and $U = 50$ V. c, d) Horizontal and vertical cross-sections through a hot spot for five supply power levels, respectively.
Rys. 3. Schemat próbki i wyniki charakteryzacji termograficznej 'wyjściowej' (niezmodyfikowanej) próbki z grafenem CVD. a) Rysunek próbki z zaznaczonym położeniem wykonanych rys. b) Obraz termiczny zasilonej próbki *wyjściowej*, $I = 30$ mA i $U = 50$ V. c, d) Odpowiednio: poziome i pionowe przekroje przez gorący punkt dla pięciu poziomów zasilania.

a)

b)
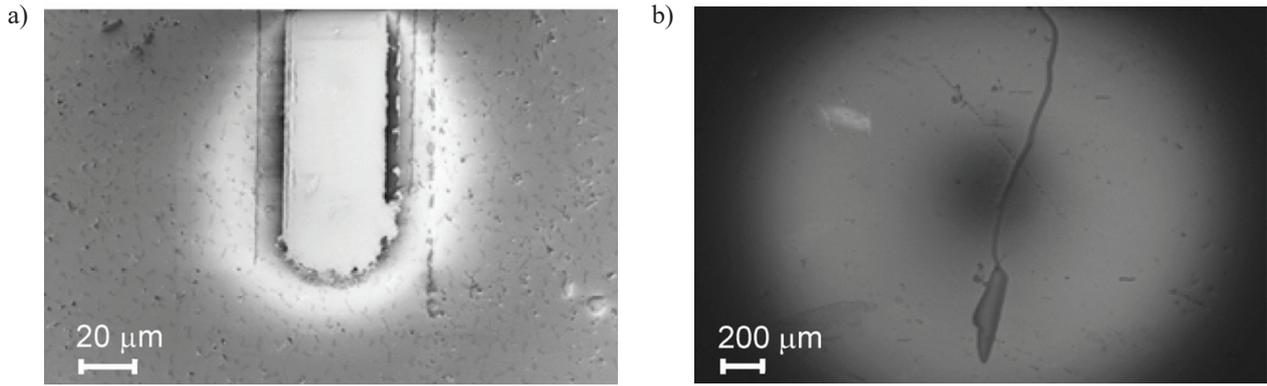
Fig. 4. SEM photographs of the graphene sample. a) Ending point of a scratch produced by nanoscratch method. b) Accidental defect on a graphene sample.

Rys. 4. Fotografia SEM próbki grafenowej. a) Końcowy fragment zarysowania wykonanego metodą nano-zarysowań. b) Przypadkowy defekt na próbce grafenowej.

a)
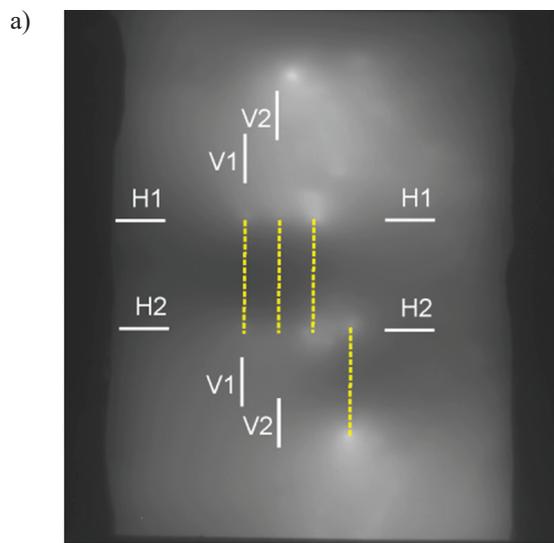
Fig. 5. Results of thermal characterization of graphene sample with intentionally introduced discontinuities. a) Thermal image for sample biased with $U = 50$ V (the position of scratches is marked with yellow dotted lines); b, c) horizontal and vertical cross-sections at marked positions, respectively.

Rys. 5. Wyniki charakteryzacji termograficznej próbki grafenowej z intencjonalnie wprowadzonymi nieciągłościami. a) Obraz termiczny zasilonej próbki, $U = 50$ V (położenie wykonanych rys zaznaczone jest żółtymi kropkowanymi liniami); b, c) odpowiednio: poziome i pionowe przekroje przez zaznaczone punkty.

b)

c)
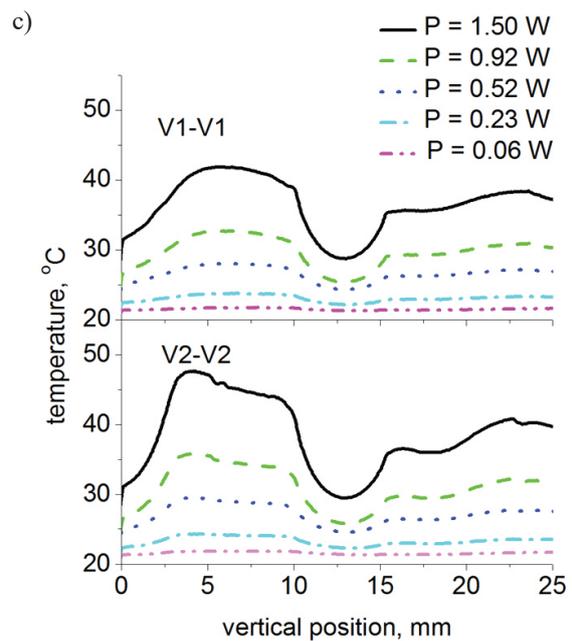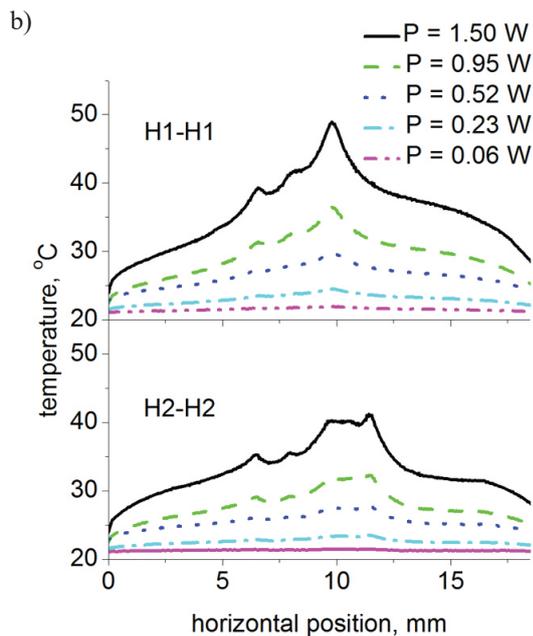
in Fig. 5a. For clarity, the positions of the scratches are marked with the dotted lines.

Horizontal cross-sections at the marked position H1-H1 and H2-H2 for five power supply levels are shown in Fig. 5b. We can see local maxima at the positions of the scratch tips. In contrast, it becomes apparent that at the horizontal cross-section H2-H2, apart from local maxima that correspond to the starting points of scratches 1, 2, 3, and ending point of scratch 4, there is a smaller peak (at horizontal position 10.6 mm) . Vertical cross-sections V1-V1 taken along scratch 1 (Fig. 5c) reveal the temperature decrease along at the scratched area and a small temperature increase at the scratch end. This effect can be observed at the cross-section V2-V2 taken along scratch 2. Here additionally, we can observe local maximum at the position 4 mm; this maximum is due to the hot spot in the upper part of the image.

To better evaluate the effect of mechanical defects on the thermal distributions, differential thermal images were calculated using thermographic camera software. These images illustrate how the thermal images of pristine sample changed due to mechanical modification of the sample. For this purpose, thermal images of pristine sample were inserted as reference images for the maps of the intentionally scratched sample (both reference and test maps were registered at the same bias level). An example of the resulting differential image for $U = 50$ V is shown in Fig. 6a. At horizontal cross-sections H1-H1 and H2-H2 (Fig. 6b), local maxima at the positions of scratch tips are clearly visible. In comparison, temperature decrease along the scratches is illustrated at vertical cross-sections V1-V1 and V2-V2 in Fig. 6c.

The results shown here clearly illustrate how alteration of current flow in a non-continuous resistive layer affects
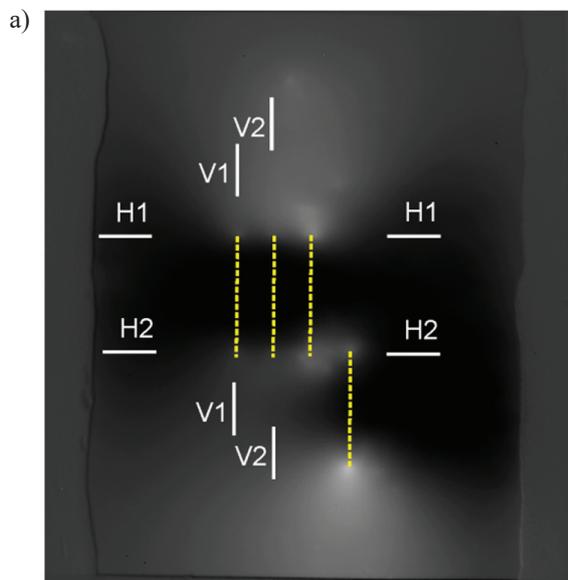
Fig. 6. Results of differential thermal measurements of graphene sample with intentionally introduced discontinuities. a) Differential thermal image for sample biased with $U = 50$ V (the position of scratches is marked with yellow dotted lines); b, c) horizontal and vertical cross-sections at marked positions, respectively.
Rys. 6. Wyniki różnicowych pomiarów termograficznych próbki grafenowej z intencjonalnie wprowadzonymi nieciągłościami. a) Różnicowy obraz termiczny zasilonej próbki, $U = 50$ V (położenie wykonanych rys zaznaczone jest żółtymi kropkowanymi liniami); b i d) Odpowiednio: poziome i pionowe przekroje przez zaznaczone punkty.
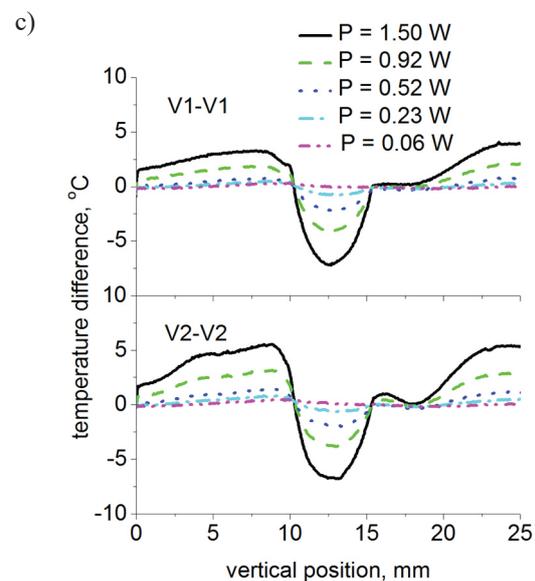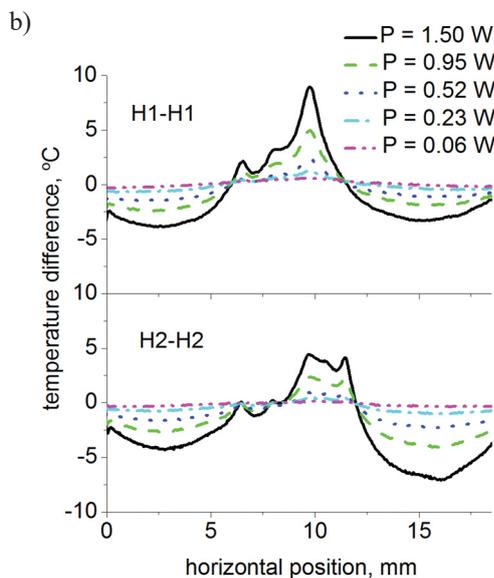
the uniformity of the resulting thermal distributions. Typically, a crack starting from the border of the sample gives a Joule heating distribution in the form of a single hot spot, whereas rectangular defects result in two hot areas at the ends of the crack [7]. These effects can be observed in Fig. 3b, Fig. 5a, and 6a. A more complicated pattern is revealed at horizontal cross-sections H2-H2 shown in Fig. 3b and 4b, where an additional maximum can be observed. A microscopic observation shows that scratch 3, presented schematically in Fig. 3a as a straight line, in practical realization forms a small zig-zag at one end. Apart from the distinct hot-spots, thermal images show overall uniform deterioration, which is probably due to layer defects such as graphene wrinkles [6], which can be frequently observed in the SEM inspection.

4. Conclusions

Our study demonstrated the influence of the intentionally and accidentally introduced discontinuities on thermal distributions of Joule-heated CVD graphene deposited on a glass sample. Such non-conductive areas can be formed during the process of deposition of graphene or during the manipulation of the samples. In spite of the theoretically high fracture strength of graphene, our results indicate high fragility of a single-layer graphene. As the tribological tests show the application of even relatively small normal loads may be destructive for graphene when applied on a small contact area. Such structural imperfections give rise to locally higher electrical fields and high local temperatures. In practice, the presented results may provide a better understanding of the heat emissions from the graphene electrodes with complex shapes. Protective layers deposited on graphene might be a good solution in many practical applications of the heaters.

Acknowledgments

References

[1] Kang J., Kim H., Kim K. S., et al: High-performance graphene-based transparent flexible heaters, *Nano Letters*, 2011, 11, 12, 5154 - 5158, 10.1021/nl202311v

[2] Kozłowska A., Kachniarz M., Gawlik G., Szewczyk R., Wojtasiak M.: Graphene Joule heating measurements in environmental chamber, *Progress in Automation, Robotics and Measuring Techniques, Advances in Intelligent Systems and Computing,* 2015, 352, 129 - 135

[3] Wróblewski G, Kiełbasiński K, Swatowska B, Jaglarz J, Marszałek K, Stapiński T, Jakubowska M.: Carbon nanomaterials dedicated to heating systems, *Circuit World*, 2015, 41, 3, 102 - 106, 10.1108/CW-05-2015-0021

[4] Bonaccorso F., Sun Z., Hasan T., Ferrari A. C.: Graphene photonics and optoelectronics, *Nature Photonics*, 2010, 4, 611 - 622, 10.1038/nphoton.2010.186

[5] Li X., Fang M., Wang W., Guo S., Liu W., Liu H., Wang X.: Graphene heat dissipation film for thermal management of hot spot in electronic device, *J. Mater. Sci.: Mater. Electron.*, 2016, 27, 7715 - 7721, 10.1007/s10854-016-4758-0

[6] Grosse K. L., Dorgan V. E., Estrada D.: Direct observation of resistive heating at graphene wrinkles and grain boundaries, *Appl. Phys. Lett.*, 2014, 105, 143109 - 143112, 10.1063/1.4896676

[7] Kozłowska A., Gawlik G., Szewczyk R., Piątkowska A., Krajewska A.: Infrared Thermal Emission from Joule-Heated Graphene with Defects, Asia Communications and Photonics Conference 2014, OSA Technical Digest, paper ATh4B.2, 10.1364/ACPC.2014.ATh4B.2

[8] Beechem T. E., Shaffer R. A., Nogan J., Ohta T., Hamilton A. B. McDonald A. E., Howell S. W.: Self-heating and failure in scalable graphene devices, *Scientific Reports,* 2016, 6:26457,1 - 7

[9] Lee C., Wei X., Kysar J. W., Hone J.: Measurement of the Elastic Properties and Intrinsic Strength of Monolayer Graphene, *Science*, 2008, 321, 385 - 388, 10.1126/science.1157996